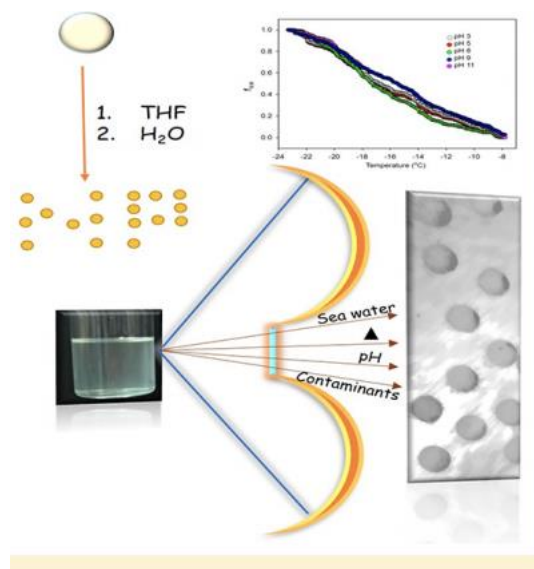# Ice Nucleation of Model Nanoplastics and Microplastics: A Novel Synthetic Protocol and the Influence of Particle Capping at Diverse Atmospheric Environments

Mainak Ganguly and Parisa A. Ariya

Abstract

Little is known about airborne atmospheric aerosols containing emerging contaminants such as nano- and microplastics. A novel, minimum energy usage, synthetic protocol of plastic micro/nanoparticles was herein developed. Stable plastic hydrosols were synthesized and characterized using three different types of plastics. The ice nucleation efficiency (INE) was investigated in both normal and synthetic seawater to mimic environmental ice nucleation. Among the three tested plastic precursors (low-density polyethylene, high-density polyethylene, and polypropylene), polypropylene produced the highest particle density with narrow particle size distribution. The change of size, shape, surface charge, and electronic behavior of the plastic nano- and microparticles accounted for the altered INE. The effects of environmental factors such as particle acidity and temperature on ice nucleation were also examined. An increase in pH increased INE due to an increased particle density (number of particles per unit volume), whereas increased temperature decreased INE significantly due to aggregation (attaching particles to produce a larger particle). Four types of capping were used on the surfaces of nano- and microplastics to investigate how the plastics act to nucleate ice when mixed with different particles. They include (a) ZnO as an emerging metal contaminant, (b) kaolin as a clay mineral, (c) $HgCl_2$ as a toxic ionic water pollutant, and (d) phenanthrene as a polycyclic aromatic hydrocarbon. Capping by ZnO and $HgCl_2$ decreased the INE of plastic nano- and microparticles, whereas kaolin and phenanthrene enhanced INE significantly. The association of contaminants to micro- and nanoplastics changes INE likely due to water affinity, surface buckling, and lattice mismatch energy of ice, affecting ice nuclei formation processes. The observed differential physicochemical behaviors of nano- and microplastics, with and without co-contaminant cappings, provide further insights to understand natural environmental ice nucleation and precipitation events. Our work shows that future emissions of nano- and microplastics may become important for cloud formation and thus anthropogenic climate change.

1. Introduction

The International Panel on Climate Change (IPCC) has reported a lack of physical–chemical understanding of airborne particulates or aerosols; their interaction with clouds is the main gap in their knowledge. Aerosol–cloud

interactions are highly uncertain in the context of estimation and interpretation of the Earth's changing energy budget.[1,2]

The research required to narrow this knowledge gap in aerosols and aerosol–cloud interactions is related to the physicochemical investigation of processes such as size, composition, configuration, contact angle, surface properties, and photochemistry.[3,4] Interestingly, similar physical and chemical properties play significant roles in the toxicological evaluation of the adverse health impact of particles. The World Health Organization (WHO) also named aerosols, especially smaller aerosols called nanoparticles (diameters <100 nm), as their top research priority and the major cause of premature human deaths globally.[5]

Progress in the development of synthetic plastics has caused an exemplar transferral in production, manufacturing, and packaging. The inexpensive and handy nature of plastics has been well appreciated in wide-ranging industries (e.g., packaging, household, automotive, electrical and electronic, construction, leisure and sports, agriculture, etc.). The production of plastic has grown exponentially and reached 335 million tons per year in 2016.[6,7]

Microplastics as well as nanoplastics are two of the evolving contaminants of global significance. Being sufficiently small, such particles may be ingested by various living organisms. As nanoplastics, they can even transverse selected biological barriers.[8] Consequently, the question of bioaccumulation and biomagnification of nano- and microplastics has recently been raised.

As synthesis of biodegradable plastics has become a rampant field of research,[6,9] there has been growing research on the potential toxicity of nano- and microplastics.[10,11] Yet, little is known about the environmental impacts of nano- and microparticles,[12] particularly in the atmosphere and atmospheric interfaces.

The presence of ice in the atmosphere can alter the energetic budget of the Earth by altering radiative properties of aerosols and aerosol–cloud interaction processes, thereby influencing climate change.[13] The Earth's precipitation mostly (more than 50%) initiates via the ice phase,[14] making atmospheric ice nucleation of the utmost importance in the global hydrological cycle.

The ice nucleation phenomenon is of two types: (a) homogeneous and (b) heterogeneous. Very low temperatures (approximately −38 °C) are required for ice formation homogeneously.[15] The ice nucleation in the natural atmosphere is virtually heterogeneous in nature. At higher temperatures, ice nucleation occurs via heterogeneous nucleation due to a reduced activation barrier (which may be explained via spherical cap formation[16,17]) caused by the presence of a so-called ice nucleating particle. In a heterogeneous ice nucleation process, the surface of the nuclei is pivotal and often determines the ice nucleation efficiency (INE) exclusively.[18−21] Ice nucleation is the first step toward the formation of a new thermodynamic phase via the self-assembly of ice embryos and determining the rate for this new phase formation. Some theoretical models explain the large variation in ice nucleation rates through the so-called "classical nucleation theory",[22] which makes an approximation of the rate at which the nucleus of a new phase formation at identical nucleation sites takes place. The rate R is described by the following equation:[23]

$$R = N_s Z j e^{-\frac{\Delta G*}{k_B T}} \tag{1}$$

where $\Delta G*$ is the Gibbs free energy at the critical radius for nucleation, k_B is the Boltzmann constant, T is the temperature at which nucleation occurs, N_s is the number of nucleation sites, Z is the Zeldovich factor (probability that the nucleus will cross the activation barrier to form a new phase rather than dissolve back into the original state), and j is the rate at which molecules attach to the nucleus, thus causing nucleic growth. The probability of nuclei formation at a specific site is proportional to the exponential term, which indicates that if $\Delta G*$ is large and positive, then the probability of nuclei formation is low, yielding a slow rate.[24]

Although heterogeneous nucleation is more common than homogeneous, homogeneous nucleation is much easier to understand from a theoretical perspective. Thus, to understand heterogeneous nucleation, one must understand homogeneous nucleation first. The classical nucleation theory derives the expression for ΔG_{HOMO} as the summation of a bulk term that is proportional to the volume of the nucleus and a surface term that is proportional to the nucleus' surface.

$$\Delta G_{HOMO} = \frac{-4}{3}\pi r^3 \Delta G_v + 4\pi r^2 \gamma \tag{2}$$

In eq 2, ΔG_V is the difference in Gibbs free energy per unit volume between the thermodynamic phase where nucleation is taking place and the phase that is nucleating, r is the nucleus radius, and γ is the surface energy/tension between the nucleus and its surroundings. According to eq 2, at very low values of r, the surface term (r^2 term)

dominates and the free energy is positive, and at higher values, the volume term (r^3 term) dominates and the free energy is negative. As the free energy is a sum of the surface and volume terms, this means that the energy goes through a maximum and the probability of nucleus formation goes through a minimum. The value of the nucleus radius at this maximum is called the critical radius. Adding new molecules to nuclei larger than this critical radius decreases the free energy, so that these nuclei become more probable to grow.[25,26]

Heterogeneous ice nucleation has been identified to proceed via four different modes (deposition ice nucleation, immersion freezing, condensation freezing, and contact freezing). Immersion freezing (starts via an ice nucleating particle immersed in a supercooled droplet) is responsible for mixed-phase cloud formation.[27,28] Investigations on the ice nucleation process reveal that water saturation is essential for ice formation in low and midlevel clouds. Thus, contact freezing or immersion freezing is pivotal. However, contact nucleation mode is less important, as thermophoretic effects help contact nucleation only in evaporating droplets, and such droplets tend to vanish before freezing.[21,29]

To understand the insight of the immersion freezing in the environment, the proxy (that mimics the environmentally available material) is often investigated in the laboratory. For example, mineral dust is considered to be a good proxy for natural dusts, subject to long-range transport. By means of laboratory proxies for natural mineral dust, instrumentation to benchmark the equipment and condition dependence of the characterized material provide a real benefit to predict the environment. A decent proxy must be a well-characterized material for environmental relevance.[21] A proxy of environmental nano- and microplastics is important to design to understand the system. Of late, researchers are trying to isolate plastic micro/nanoparticles from the environment and studying their physicochemical properties.[30,31] However, the synthesis of nano- and microplastic particles in the laboratory for a better understanding of their properties has been quite uncommon until now. Recently, Balakrishnan et al.[32] synthesized polyethylene micro/nanoparticles in toluene using biosurfactant.

Yearly plastic manufacturing presently exceeds 380 million tons, summing up to 8300 million tons produced until 2015.[33] Roughly, 39.9% of it came from packaging.[34] Nano- and microplastic is often believed as a never-ending boomerang tale. On the Pyrenees Mountains (southern France), scientists noted a daily rate of 365 microplastic particles per square meter dropping from the sky.[35] Thus, the influence of nano- and microplastics on the atmosphere, especially on the ice nucleation process, is pivotal.

Research on nano- and microplastics is going to be an emerging field in the near future, considering the impact on the environment and human health. Collection of plastic micro/nanoparticles from the atmosphere has been attempted in some cases to investigate their role on our environment.[36,37] However, such studies are highly site-dependent, providing narrow fundamental knowledge. To understand the system better, we considered producing nano- and microplastics in the laboratory in an energy-efficient way. We also explored the effects of several environmental factors (temperature, acidity, and various aquatic media including seawater) on the ability of nano- and microplastics to nucleate ice in the immersion mode. Furthermore, to evaluate the ice nucleation of mixed particles containing nano- and microplastics, we performed experiments using four different types of capping at near environmentally relevant conditions.

2. Experimental Section

2.1. Materials and Supplies

All of the used reagents were of analytical reagent (AR) grade, and milli-Q water was used throughout the experiment. Low-density polyethylene (1000 μm) [product number 43949-18] and high-density polyethylene (MW 125000) [product number 41731-30] were purchased from Alfa Aesar. Polypropylene (MW ∼ 12000) [product number 428116-250G] and artificial seawater [product number SSWS30-10x30ML] (composition is discussed later) were acquired from Sigma-Aldrich. Hydrochloric acid, sodium hydroxide, and tetrahydrofuran were obtained from Fisher Scientific. All glassware was cleaned with freshly prepared aqua regia and subsequently rinsed with copious amounts of distilled water and dried well before use. All reagents were used without further purification.

2.2. Synthesis of Nano- and Microplastics

A bead of high-density polyethylene (HDPE), having a mass of 105 mg, was shaken (100 rpm) for 48 h in 100 mL of tetrahydrofuran (THF) at room temperature. Subsequently, the bead of HDPE was separated from THF. We thus obtained THF, saturated with HDPE. The dissolved HDPE was calculated by measuring the mass difference of the

bead before and after THF treatment. We found that 5 mg of HDPE was dissolved in 100 mL of THF. Finally, 1 mL of THF, saturated with HDPE was mixed thoroughly with 9 mL of water to obtain plastic hydrosol (HDPEH). The same experiment was done for low-density polyethylene (LDPE) and polypropylene (PP). After saturation of THF with HDPE and PP, we diluted them by THF to obtain 5 mg of HDPE and PP in 100 mL of THF. Subsequently, 1 mL of LDPE/THF solution was mixed with 9 mL of water to obtain LDPEH. Likewise, 1 mL of PP/THF solution was mixed with 9 mL of water to obtain PPH.

2.3. Analytical Techniques for Physical and Chemical Characterization

2.3.1. UV–Vis Spectroscopy

All UV–vis absorption spectra of the 3.5 mL sample solution were obtained on a Varian Cary 50 Bio UV spectrophotometer, using a quartz cuvette.

2.3.2. Transmission Electron Microscopy

Samples were vacuum-dried at room temperature before measurement. The samples were put on a carbon tape before TEM analyses. Ten microliters of each sample solution was subsequently deposited on glow-discharged carbon-film-coated copper electron microscopy grids and dried. The samples were imaged using a FEI Tecnai 12 Biotwin TEM microscope (FEI Electron Optics) equipped with a tungsten filament at 120 kV, containing an AMT XR80C CCD camera system.

2.3.3. Nanoparticle Tracking Analysis

The hydrodynamic size distributions of hydrosols were measured by nanoparticle tracking analysis (NTA), using a Malvern NanoSight NS500 with a laser wavelength of 532 nm and an electron multiplying charge coupled device camera. The average of the three measurements is reported.

2.3.4. Drop Freezing Assays

Nano- and microplastics were suspended in water, making hydrosols. Subsequently, hydrosols were aged at different conditions (T, pH, composition, etc.). Afterward, they were sonicated for 20 min prior to the ice nucleation experiments. For each sample, 10 μL of 200 droplets was placed on a cooling plate (in-house-made copper plate), and the plate (starting at ∼0 °C) was cooled at a rate of 1 °C/min. The temperature at which each droplet froze was observed by the naked eye and recorded. Before the droplets were added, a thin layer of petroleum jelly was spread on the copper plate to minimize the reactions between the copper plate and the drops in addition to maintaining hydrophobicity. Milli-Q water was used as diluent, and control ice nucleation plots are included in Figure S1 of the Supporting Information.

The process of immersion ice nucleation in a supercooled drop was quantified via active site density per unit mass. The cumulative number of ice nucleation active sites per unit volume of water (K) at a certain temperature (T) can be obtained by the following equation.

$$K(T) = \frac{-\ln\left(1 - f_{ice}(T)\right)}{V} \tag{3}$$

where f_{ice} is the fraction of frozen droplet and V is the volume of a droplet.

As we know the mass of particles per unit volume of water, the ice nucleation active site density per unit mass (n_m) was expressed as follows

$$n_m(T) = \frac{[K(T)d]}{C_m} \tag{4}$$

C_m denotes the mass concentration of the particles in the initial suspension, and d represents the dilution ratio of the suspension relative to C_m. Error bars represent the standard deviation after three measurements of the active site density.

The T_{50} value defines the temperature at which 50% of the observed droplets are frozen.[38] T_{50} values, reported here, are the averages of three experiments.

3. Results and Discussion

We considered HDPE (that is a very common form of plastic in our day to day life)[37] as one of the studied compounds and performed detailed analysis of it in the context of plastic nano- and microparticles, which contain this compound. Please note that we also synthesized and performed additional experiments regarding their INE ability for other forms of plastic nano- and microparticles at different conditions. The other types of plastic particles included both PP and LDPE, as described in the abstract, in the Experimental Section, as well as here in the Results and Discussion.

3.1. Characterization of HDPEH

To understand the INE of nano- and microplastics as an environmental proxy, good characterization was pivotal. As THF is an inorganic Lewis base, the negative surface charge on the plastic nano- and microparticles exhibited a repulsive force between each other, responsible for the stability of the white plastic hydrosol. In other words, nano- and microparticles were stable as a suspended state in water due to THF capping. By replacing the HDPE precursors with PP, we could achieve tight size distributions (discussed later) of nano- and microplastics. SAED (selected area electron diffraction)[39] indicated that the particles had a good amount of crystallinity.

Baruah et al.[40] synthesized ZnO@polyethylene, and the lattice fringe was determined to be ∼0.33 nm. It might be due to the wurtzite structure of ZnO or polyethylene (not considered in their study). Again, the (002) plane of graphite was reported to be 0.34 nm.[41] We observed, in the present study, a prominent lattice fringe of plastic particles of 0.345 nm, as found from high-resolution transmission electron microscopy (HRTEM) analysis. Hence, one might consider that the decently crystalline[42] plastic nano- and microparticles synthesized in this study were comparable to graphite (Figure 1).
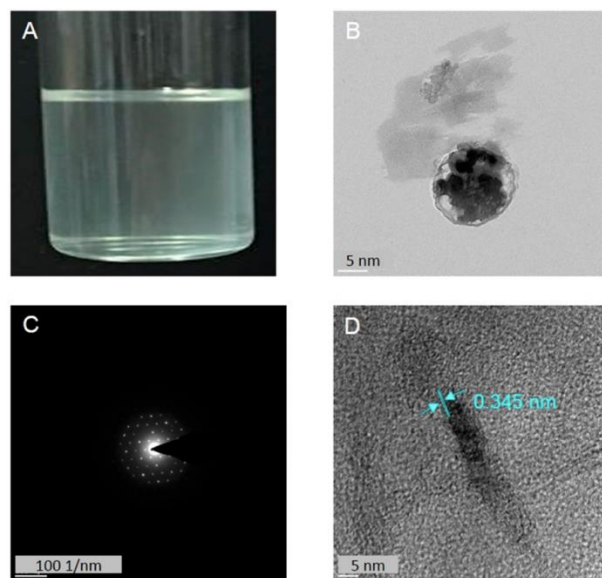

Figure 1. (A) Digital image, (B) TEM, (C) SAED, and (D) HRTEM image of HDPEH.

When 1 mL of saturated solution of HDPE in THF was added to 9 mL of water, plastic hydrosol HDPEH was obtained. The particles in HDPEH were mostly ∼118 nm in size, and particles of larger size were also available to some extent, as obtained from NTA analyses (Figure 2).
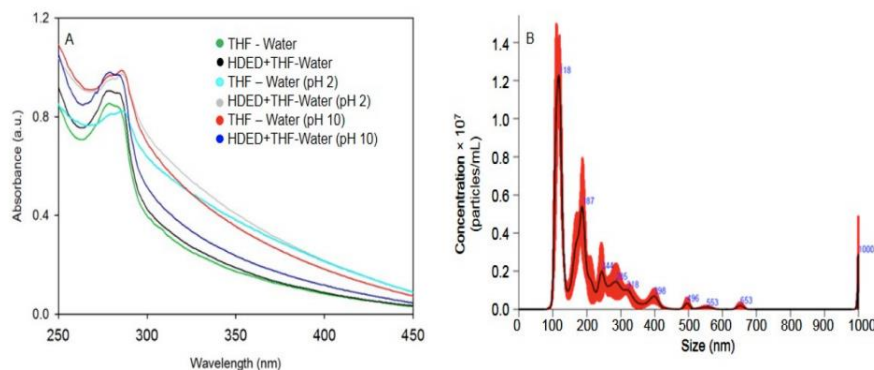
Figure 2. (A) UV−vis spectra of HDPEH at different pH values and (B) particle size density of HDPEH at pH 8.

The UV–vis absorption spectrum of pure THF in water showed two overlapping peaks with maxima at 277 and 284 nm. Such peaks enhanced their absorbance of 7% with just 1 nm red shift due to the association of plastic molecules to THF to form nano- and microplastics. THF helped to cap plastic particles to be stable as hydrosol.

3.2. Effect of pH on HDPEH

As THF is a Lewis base with a lone pair of electrons, the HDPEH was alkaline (pH 8). We further changed the pH by adding NaOH and HCl. At pH 3, particles are mostly around ∼277 nm in size. A wide distribution was obtained between 100 and 400 nm at pH 11 (Figure 3). However, from TEM images, it was found that particles of HDPEH in highly acidic pH (3) were smaller (or fragmented) than those in highly alkaline pH (11).
For both cases, the SAED image indicated the crystallinity of the materials, yet the distorted sphere of SAED implied the low melting materials (corroborating the plastic materials).
We were also able to detect the lattice fringe of HDPEH particles at 0.252 nm at pH 3 (Figure 4). This is for the (102) plane of sp^2 graphitic carbon, as reported by Wang et al.[43] The absorbance of the peak of THF at 286 nm was enhanced noticeably (18%) at pH 3 of the HDPEH solution due to the formation of nano- and microplastics (although the absorption maximum remained virtually unchanged). An approximate 8 nm blue shift was noticed at pH 11 for HDPEH (Figure 2A).
The ice nucleation efficiency was increased by both increasing as well as decreasing the pH of HDPEH due to higher particle density. At higher and lower pH, the particle density was increased, providing more surfaces to nucleate, therefore, accounting for the high INE. From NTA, we found that 4.87×10^8/mL, 3.91×10^8/mL, and 1.59×10^9/mL were the particle densities at pH 3, pH 8, and pH 11, respectively. Hence, pH 11 had a remarkably high particle density in comparison to that of other pH values used in this study, and it also exhibited the highest observed INE.
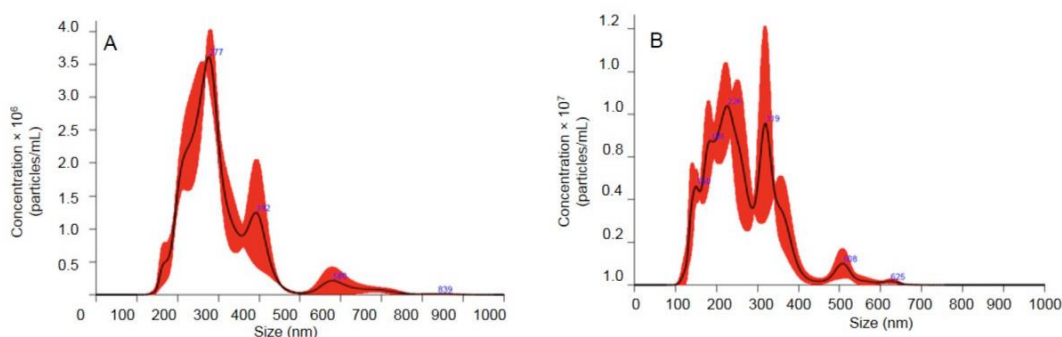

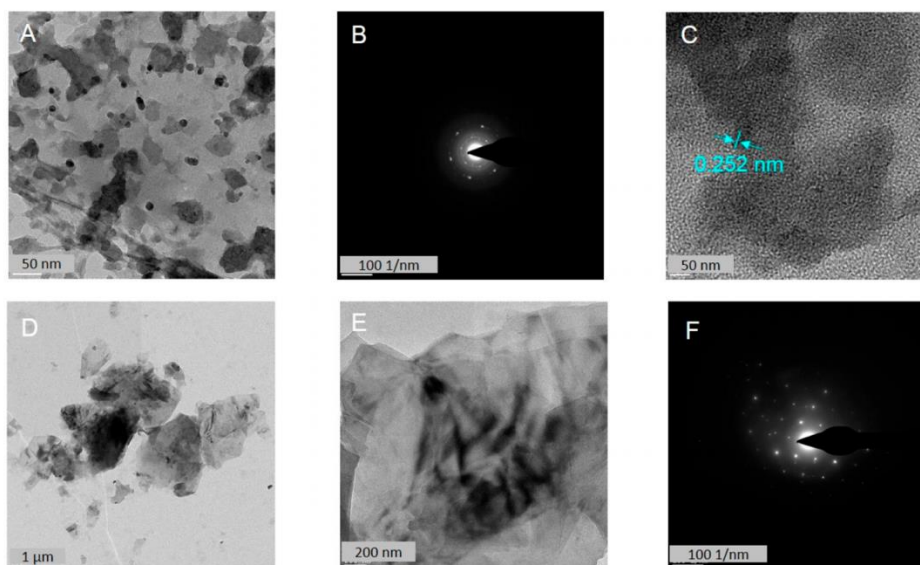**Figure 3.** Particle size density of HDPEH at (A) pH 3 and (B) pH 11.

Figure 4. (A) TEM, (B) SAED, and (C) HRTEM image of HDPEH at pH 3; (D) TEM, (E) another TEM, and (F) SAED image of HDPEH at pH 11.

3.2.1. Effect of pH on the INE

The T_{50} of HDPEH was −16.2, −17.3, and −15.2 °C at pH 3, pH 8, and pH 11, respectively. It is well-established that by increasing the surface area the ice nucleation ability of a particle type should increase.(44−47) However, nano- and microplastics discussed in the present paper are hydrosol and very dilute. If we dry the hydrosol to measure the surface area (Brunauer–Emmett–Teller analysis etc.), the actual surface will be highly compromised due to aggregation, providing unreliable information on ice nucleation. To make the comparison, we calculated active site density per unit mass (Figure 5), as reported by Tobo et al.(44) Experiments were conducted a minimum of three times. Thus, the result clearly depicted the different INE of various types of plastic nano- and microparticles.

Although the ice nucleation plots might look similar, different T_{50} values justify that the changes in the fragmented/aggregation state or the size distribution of the plastic had some influence on the INE. Moreover, the range of freezing temperature was different for each case. That was reflected in the T_{50} values (Figure 5.)
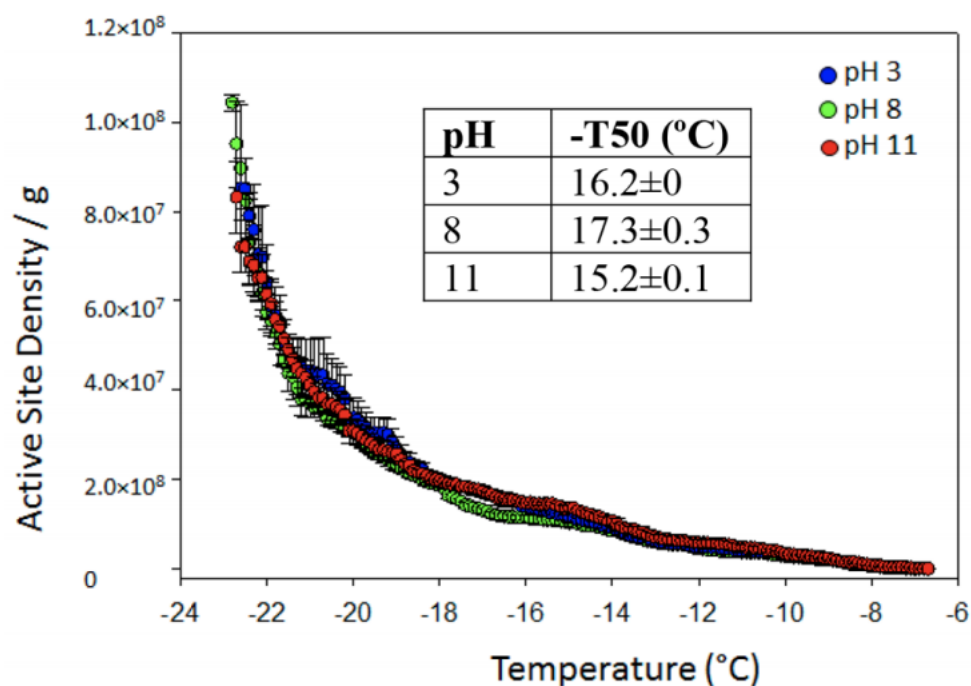
Figure 5. Freezing spectra of HDPEH at various pH values.

3.3. Effect of Temperature on HDPEH

Enhanced temperatures might remove THF capping, destabilizing the system. Low melting behavior should also be considered in this regard. NTA analysis revealed that most of the particles were ~119 and ~177 nm in size (with a range of 100–300 nm). TEM imaging indicated the aggregated nature of the particles, whereas HRTEM indicated 0.361, 0.331, and 0.356 nm (sp^2 graphitic lattice fringe, as mentioned earlier). In a fixed region, the variable lattice fringes and nonprominent SAED image were indications of poor crystallinity (due to heating) (Figure 6).
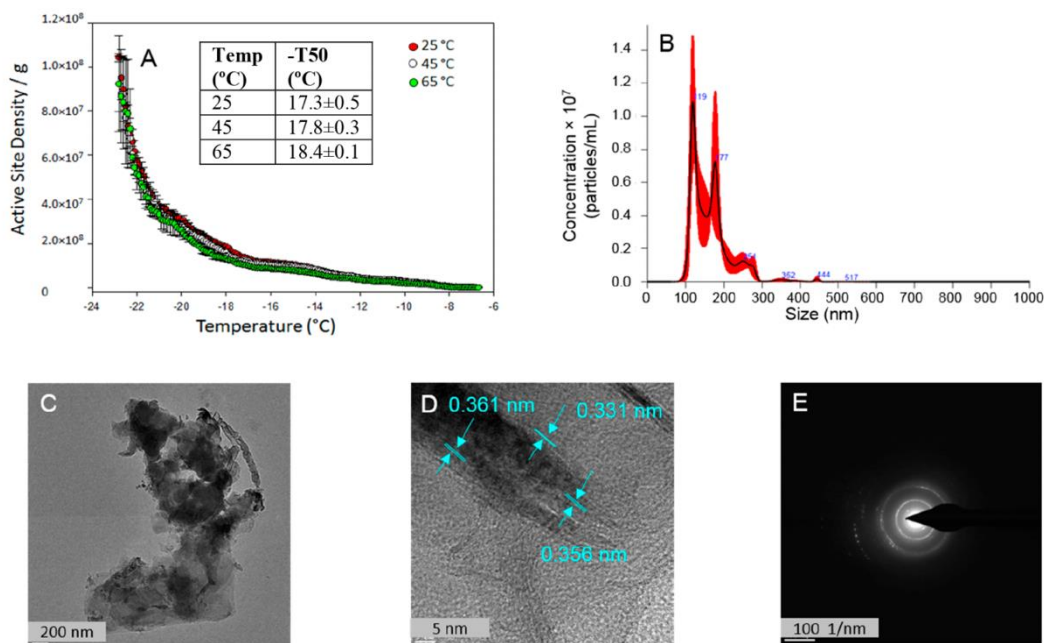
Figure 6. (A) Ice nucleation spectra of HDPEH after aging 1 h at different temperature. (B) Particle size density, (C) TEM, (D) HRTEM, and (E) SAED image of HDPED after being aged for 1 h at 40 °C.

3.3.1. Effect of Aging at Different Temperatures on INE

As plastic is a low melting material, the heating of HDPEH influenced ice nucleation ability, concerning size, shape, morphology, etc. T_{50} was found to be −17.3, −17.8, and −18.4 °C when HDPEH was aged at 25, 45, and 65 °C, respectively, for 1 h (Figure 6). It was reported by Oliani et al.(48) that the decrease of the crystalline phase of high melt strength polypropylene takes place owing to chain scission mechanisms on thermal aging. Contraction of the surface layers is a consequence of chemicrystallization and results in surface cracks.

The observed changes in INE at increased temperatures of nano- and microplastics was likely due to alterations of crystallinity. Chong et al.(42) have recently reported the influence of crystallinity as well as crystal structure on the immersion freezing of alumina. Hence, we expect that change in crystallinity is a factor to alter INE. In this study, increased temperature caused only a little permanent change in crystallinity of plastic nano- and microparticles, with little change of INE.

3.4. Other Precursors To Obtain Plastic Nano- and Microparticles

Various types of plastics are used in our daily life.(37) In the aforementioned section, the physicochemical properties including ice nucleation behavior(27,28) of nano- and microplastics in HDPEH prepared from HDPE were discussed. However, we also synthesized plastic hydrosol LDPEH and PPH from low-density polyethylene (LDPE) and PP, respectively. NTA analyses revealed that particles in LDPEH were from 100 to 800 nm, that is, a wide range of size distribution. On the other hand, PPH possessed a highly tight size distribution (67–383 nm), and maximum particles were ∼193 nm (Figure 7). The experimental conditions used in this study were highly suitable for polypropylene to generate particles of precise sizes. The particle densities in HDPEH, LDPEH, and PPH were shown to be 3.91×10^8, 2.60×10^8, and 1.55×10^{10}/mL. PP produced, once again, a significantly higher number of particles in comparison to other precursors. Frei et al.(49) have reported the responses of plastic at increased temperatures. Here, we studied the effect on INE of nano- and microplastics due to thermal aging.
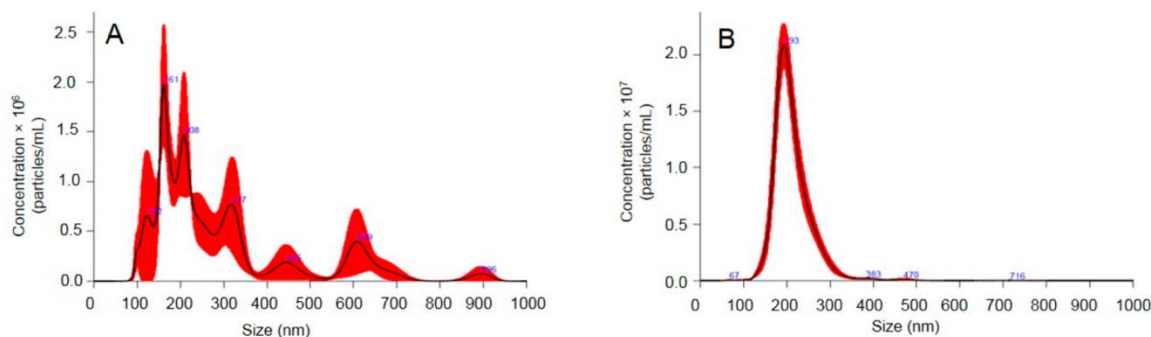
Figure 7. Particle size density spectra of (A) LDPEH and (B) PPH.

3.5. Effect of Suspension in Seawater on INE: Comparison of INE between Different Synthetic Methods of the Plastics

We investigated the effect of seawater on ice nucleation. Hence, we used artificial seawater (Paragon Scientific) in lieu of milli-Q water. Artificial seawater contains NaCl (24.53 g/L), MgCl$_2$ (5.20 g/L), Na$_2$SO$_4$ (4.09 g/L), CaCl$_2$ (1.16 g/L), KCl (0.695 g/L), NaHCO$_3$ (0.201 g/L), KBr (0.101 g/L), H$_3$BO$_3$ (0.027 g/L), SrCl$_2$(0.0025 g/L), NaF (0.003 g/L), and water (988.968 g/L).[50] Artificial seawater is often used to have a comprehensive knowledge of ice nucleation microphysics in the real environment. Junge and Swanson reported high-resolution ice nucleation spectra from sea-ice bacteria using artificial seawater.[51] Depression of freezing point due to the salts in seawater is also known.[52] We plotted active site density per unit mass with error bars with plastic particles (Figure 8). We used the total mass of the solute-suspended materials in water to prepare the active site density per unit mass. Control experiments was also performed (Figure S1, Supporting Information).

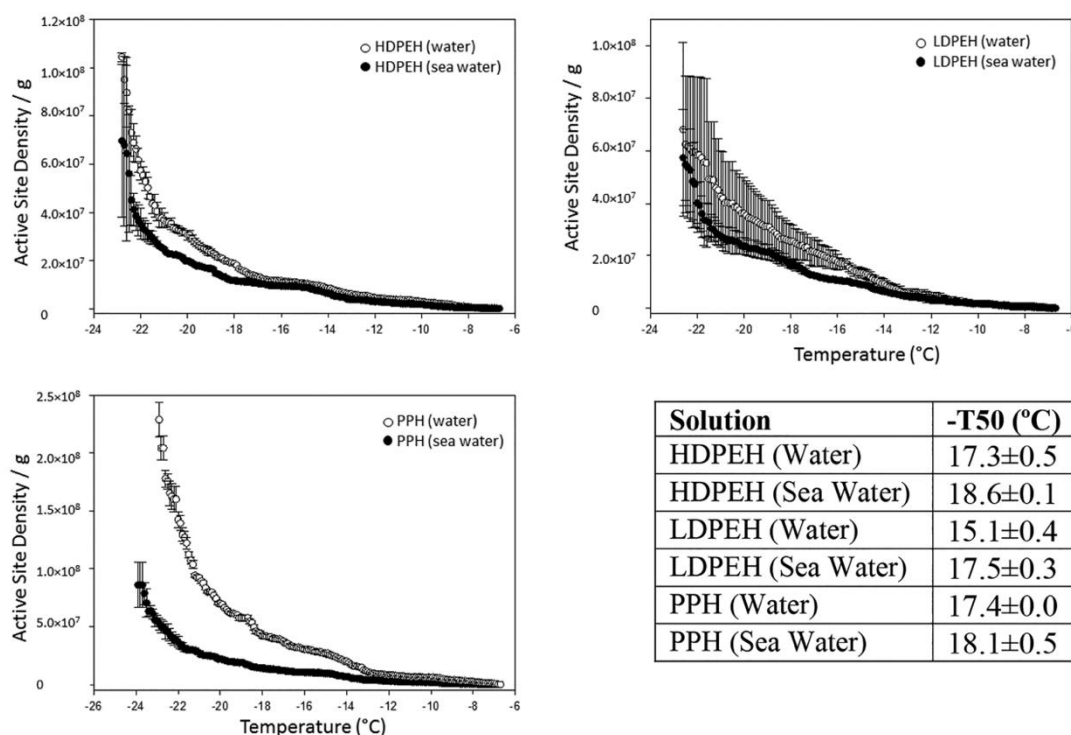| Solution	-T50 (°C)
HDPEH (Water)	17.3±0.5
HDPEH (Sea Water)	18.6±0.1
LDPEH (Water)	15.1±0.4
LDPEH (Sea Water)	17.5±0.3
PPH (Water)	17.4±0.0
PPH (Sea Water)	18.1±0.5

Figure 8. Ice nucleation spectra of plastic hydrosols from different precursors, both in water and in seawater.

We observed that the ice nucleation efficiency was decreased noticeably in artificial seawater for all HDPEH, LDPEH, and PPH. T_{50} was −17.4, −15.1, and −17.3 °C for PPH, LDPEH, and HDPEH, respectively, when the medium was pure water. On the contrary, T_{50} was −18.1, −17.5, and −18.6 °C for PPH, LDPEH, and HDPEH,

respectively, when the medium was seawater. Ice nucleation is generally favored by water affinity, low lattice mismatch, and surface buckling of the ice nucleating particles.[53] The various constituents of artificial seawater as a whole disfavored any one/all of the factors, rendering decreased ice nucleation ability.

3.6. Effect of Co-contaminants on INE of Nano- and Microplastics: Comparison of INE between Different Synthetic Methods of the Plastics

As nano- and microplastics are abundant in our atmosphere,[54] they can be capped with other contaminants to alter the ice nucleation efficiency. We chose four very common contaminants: (a) ZnO as an emerging metal contaminant, (b) kaolin as a clay mineral, (c) $HgCl_2$ as a toxic ionic water pollutant, and (d) phenanthrene as a polycyclic aromatic hydrocarbon.

ZnO is one very common emerging contaminant, released from sunscreen products, cosmetics, pigments, industrial coatings, plastic additives, semiconductors, textiles, and antibacterial agents.[55] Widespread applications of ZnO also include toxicity[56] in humans and ecology.[57] We investigated the effect of ZnO on the ice nucleation ability of plastic nano- and microparticles in PPH, LDPEH, and HDPEH. Interestingly, INE of ZnO was decreased significantly in the presence of nano- and microplastics. T_{50} was −16.0 °C for ZnO in water, −18.0 °C for ZnO in PPH, −17.6 °C for ZnO in LDPEH, and −19.4 °C for ZnO in HDPEH. There are rarely any reports so far for heterogeneous ice nucleation in the immersion mode of ZnO. We reported previously[58] that ZnO reduced INE of purely inorganic and environmentally available ice nucleating particles. In this study, we found that plastic nano- and microparticles decreased the INE of ZnO.

Kaolin is one of the most widely abundant clay minerals. The mechanistic ground of ice nucleation is not fully understood. Hence targeted, atmospherically relevant ice nucleation studies[59] are important. They can contribute further physicochemical understanding of ice nucleation, which is one of the major uncertainties in the quantification of the magnitude of climate change. We investigated the INE of kaolin in the presence of nano- and microplastics and observed that INE was increased, being associated with plastic. T_{50} was −19.0 °C for kaolin in water, −17.0 °C for kaolin in PPH, −15.9 °C for kaolin in LDPEH, and −16.2 °C for kaolin in HDPEH. Wex et al.[60] reported the different extents on INE of kaolin particles from different coatings (organic as well as inorganic). Here, kaolin being passivated with plastic enhanced INE significantly. It is possible that this observation is related to changes of the layered structures of kaolin.
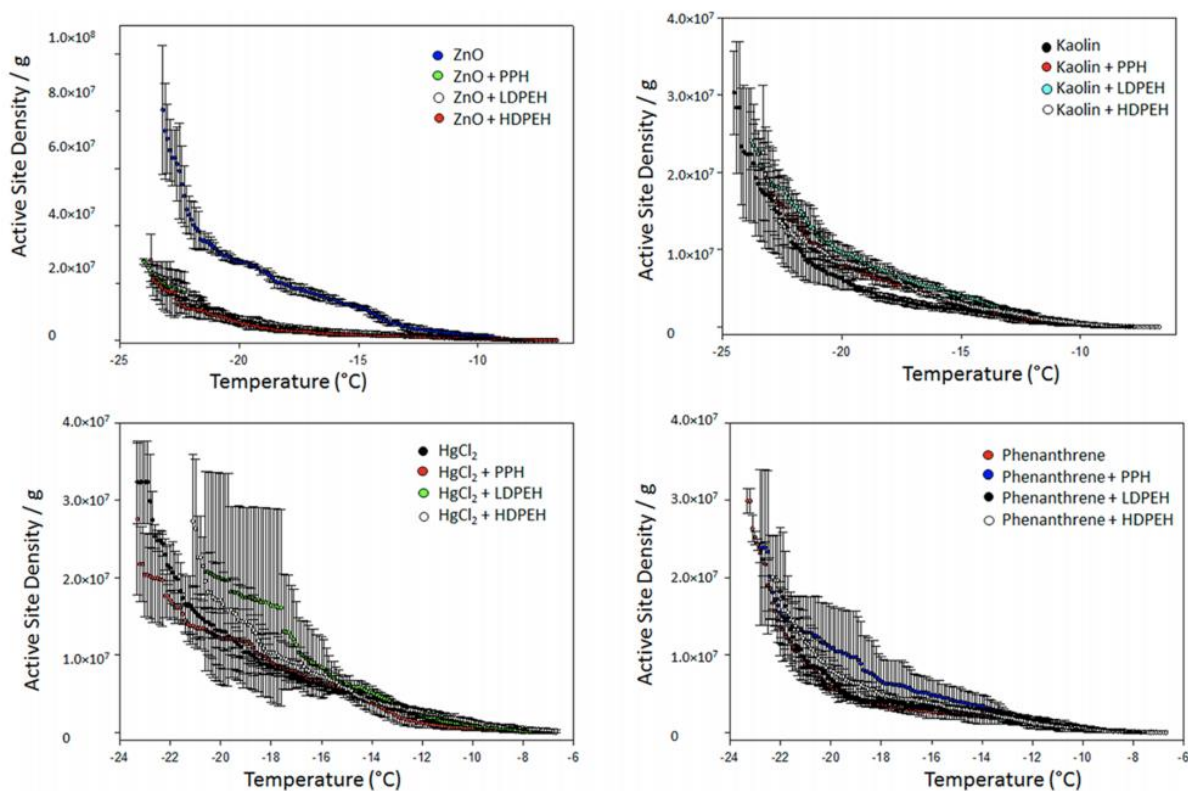
$HgCl_2$, available in the air and water, affects not only human health but also environmental health and climate.[61−63] $HgCl_2$, being attached to nanocomposites, dramatically alters INE. Previously, we have reported that in the presence of $HgCl_2$, maghemite ice nucleating efficiency improved significantly.[61] However, in the present study, plastic nano- and microparticles are shown to decrease INE of $HgCl_2$, likely by changing the water affinity. It was observed that T_{50} was −14.3 °C for $HgCl_2$ in water, −14.5 °C for $HgCl_2$ in PPH, −13.9 °C for $HgCl_2$ in LDPEH, and −16.6 °C for $HgCl_2$ in HDPEH solutions.

Polycyclic aromatic hydrocarbons (PAHs), a class of organic molecules, are usually fused aromatic type rings. They are highly noxious as well as carcinogenic micro-organic pollutants. Natural as well as anthropogenic events (e.g., bush fires, combustion of fossil fuels, military operations, agriculture, residential waste burning, vehicular emissions, leakages from the petroleum industry, manufacturing of carbon black, heating and power generation, coal tar pitch and asphalt, and emissions from internal combustion engines) produce PAH.[64] There are 16 PAH compounds in the EPA priority list.[65] Phenanthrene is one of them. T_{50} was −19.4 °C for phenanthrene in water, −17.4 °C for phenanthrene in PPH, −19.1 °C for phenanthrene in LDPEH, and −18.0 °C for phenanthrene in HDPEH. Therefore, it was evident that nano- and microplastics increased the INE of phenanthrene.

Depending on the nature of the contaminants, INE may thus be increased or decreased in the presence of nano- and microplastics (Figure 9). Plastic is a hydrophobic material, having adverse effects on ice nucleation (according to the classical nucleation theory). Electron microscopy imaging did not indicate the roughness of the plastic particles. Therefore, it is likely that a mechanism related to the low lattice mismatch between ice and plastic particles is attributed to enhancement of INE.[58,61]

The difference of the INE of plastic particles with several contaminants was likely the outcome of the above factors. We herein investigated three types of plastic particles at various conditions to understand the tentative effect of the nano- and microplastics in the atmosphere in the context of INE. The extensive use of plastic materials in Earth's environment produces diverse types of nano- and microplastics, which can undergo further transformation. The existence of plastic nano- and microparticles may drive additional physicochemical interactions with other natural or anthropogenic contaminants in the atmosphere. This might affect the ice nucleation processes of aerosols and the formation of novel types of clouds in terms of compositions and phases (i.e., mixed-phase clouds).

The environmental fate of microplastic and nanoplastic is not limited to ice nucleation. Their potential impacts in both marine and terrestrial ecosystems have been proposed.(66,67) However, there are still several unknowns. The majority of human populations live in cities where there are significant plastic emissions and sinks of emerging plastic contaminants.(68) Hence, further impact studies are recommended to evaluate the potential impact of nano- and microplastics on biogeochemical processes, including in urban areas.

Material	T50 (^{0}C)	Material	T50 (^{0}C)	Material	T50 (^{0}C)	Material	T50 (^{0}C)
ZnO (Control)	-16.0	Kaolin (Control)	-19.0	HgCl$_2$ (Control)	-14.3	Phenanthrene (Control)	-19.4
ZnO + PPH	-18.0	Kaolin + PPH	-17.0	HgCl$_2$ + PPH	-14.5	Phenanthrene + PPH	-17.4
ZnO + LDPEH	-17.6	Kaolin + LDPEH	-15.9	HgCl$_2$ + LDPEH	-13.9	Phenanthrene + LDPEH	-19.1
ZnO + HDPEH	-19.4	Kaolin + HDPEH	-16.2	HgCl$_2$ + HDPEH	-16.6	Phenanthrene + HDPEH	-18.0

Figure 9. Ice nucleation spectra of ZnO, kaolin, HgCl$_2$, and phenanthrene in water (with THF, control), PPH, LDPEH, and HDPEH. Tabular representation of T_{50} of different contaminants with nano- and microplastics.

4. Conclusions

This is the first report of the laboratory synthesis of nano- and microplastics in the context of ice nucleation. The synthetic protocol was also found to be energetically efficient. The responses of them on several physicochemical conditions, along with common contaminants, were noteworthy. Interactions of ZnO and $HgCl_2$ decreased INE of plastic micro/nanoparticles, whereas kaolin and phenanthrene increased INE appreciably. The change of size, shape, surface chemistry, and electronic behavior of plastic nanoparticles are often considered as causes for the altered INE.(58,61,69) These physicochemical factors are likely to be the cause of the alteration of the ice nucleation properties of the plastic particles used in this study. However, we recommend additional research to determine which of these factors or combination of them is predominantly responsible for exhibited nano- or microplastic ice nucleation. This work may open up a facet on the role of airborne nanoparticles in climate change and cloud formation. We speculate that selected plastic nano- or microparticles can undergo microbiological or biological transformation, similar to several known organic compounds in the environment.(70−72) Thereby, further bio-geochemical transformations may alter ice nucleation abilities at different environmental conditions.

Further study is warranted for establishing an unequivocal mechanism for synthetic nano- and microplastic-induced nucleation to correlate with the effect of environmental ultrafine plastic. Moreover, the hydrophobic nature combined with a huge surface area of such tiny particles in micro/nano regimes may be an asset to design smart materials to decontaminate seawater from organic contaminants, namely, mineral oil.

Supporting Information

The Supporting Information is available free of charge on the ACS Publications website at DOI: 10.1021/acsearthspacechem.9b00132.

Author Information

Corresponding Author
Parisa A. Ariya - *Department of Atmospheric and Oceanic Sciences, McGill University, Montreal, Quebec H3A 0B9, Canada*; *Department of Chemistry, McGill University, Montreal, Quebec H3A 0B8, Canada*; http://orcid.org/0000-0001-5269-5017; Email: parisa.ariya@mcgill.ca
Author
Mainak Ganguly - *Department of Atmospheric and Oceanic Sciences, McGill University, Montreal, Quebec H3A 0B9, Canada*; http://orcid.org/0000-0002-5315-7381
Notes
The authors declare no competing financial interest.

Acknowledgments

(1) https://www.ipcc.ch/2015/ (accessed May 14, 2019).

(2) https://apps.who.int/iris/bitstream/handle/10665/272596/ 9789241565585-eng.pdf (accessed May 14, 2019).

(3) Fan, J. W.; Wang, Y.; Rosenfeld, D.; Liu, X. H. Review of aerosol- cloud interactions: mechanisms, significance, and challenges. *J. Atmos. Sci.* 2016, *73*, 4221−4252.

(4) Giorio, C.; Monod, A.; Brégonzio-Rozier, L.; DeWitt, H. L.; Cazaunau, M.; Temime-Roussel, B.; Gratien, A.; Michoud, V.; Pangui, E.; Ravier, S.; et al. Cloud processing of secondary organic aerosol from isoprene and methacrolein photooxidation. *J. Phys. Chem. A* 2017, *121*, 7641−7654.

(5) Slezakova, K.; Morais, S.; Carmo Pereir, M. d. Atmospheric Nanoparticles and Their Impacts on Public Health. *Current Topics in Public Health* 2013, 54775.

(6) Taniguchi, I.; Yoshida, S.; Hiraga, K.; Miyamoto, K.; Kimura, Y.; Oda, K. Biodegradation of PET: Current Status and Application Aspects. *ACS Catal.* 2019, *9*, 4089−4105.

(7) PlasticsEurope Plastics - the Facts 2017: An Analysis of European Plastics Production, Demand and Waste Data; https://www.plasticseurope.org/application/files/5715/1717/4180/Plastics_   the_facts_2017_FINAL_for_website_one_page.pdf (accessed Jan 30, 2019).

(8) Ng, E.-L.; Huerta Lwanga, E.; Eldridge, S. M.; Johnston, P.; Hu, H.-W.; Geissen, V.; Chen, D. An overview of microplastic and nanoplastic pollution in agroecosystems. *Sci. Total Environ.* 2018, *627*, 1377−1388.

(9) Mostafa, N. A.; Farag, A. A.; Abo-Dief, H. M.; Tayeb, A. M. Production of biodegradable plastic from agricultural wastes. *Arabian J. Chem.* 2018, *11*, 546−553.

(10) Revel, M.; Chátel, A.; Mouneyrac, C. Micro(nano)plastics: A threat to human health? *Current Opinion in Environmental Science & Health* 2018, *1*, 17−23.

(11) Lehner, R.; Weder, C.; Petri-Fink, A.; Rothen-Rutishauser, B. Emergence of Nanoplastic in the Environment and Possible Impact on Human Health. *Environ. Sci. Technol.* 2019, *53*, 1748−1765.

(12) Burns, E. E.; Boxall, A. B. A. Microplastics in the Aquatic Environment: Evidence for or against Adverse Impacts and Major Knowledge Gaps. *Environ. Toxicol. Chem.* 2018, *37*, 2776−2796.

(13) Knopf, D. A.; Alpert, P. A.; Wang, B. The Role of Organic Aerosol in Atmospheric Ice Nucleation: A Review. *ACS Earth Space Chem.* 2018, *2*, 168−202.

(14) Lau, K. M.; Wu, H. T. Warm rain processes over tropical oceans and climate implications. *Geophys. Res. Lett.* 2003, *30*, 2290.

(15) Heymsfield, A. J.; Miloshevich, L. M. Homogeneous Ice Nucleation and Supercooled Liquid Water in Orographic Wave Clouds. *J. Atmos. Sci.* 1993, *50*, 2335−2353.

(16) Cabriolu, R.; Li, T. Ice Nucleation on Carbon Surface Supports the Classical Theory for Heterogeneous Nucleation. *Phys. Rev. E* 2015, *91*, 052402.

(17) Khvorostyanov, V. I.; Curry, J. A. The Theory of Ice Nucleation by Heterogeneous Freezing of Deliquescent Mixed CCN. Part I: Critical Radius, Energy, and Nucleation Rate. *J. Atmos. Sci.* 2004, *61*, 2676−2691.

(18) Zhang, X. − X.; Chen, M.; Fu, M. Impact of surface nanostructure on ice nucleation. *J. Chem. Phys.* 2014, *141*, 124709.

(19) Reinhardt, A.; Doye, J. P. K. Effects of surface interactions on heterogeneous ice nucleation for a monatomic water model. *J. Chem. Phys.* 2014, *141*, 084501.

(20) Cox, S. J.; Raza, Z.; Kathmann, S. M.; Slater, B.; Michaelides, A. The microscopic features of heterogeneous ice nucleation may affect the macroscopic morphology of atmospheric ice crystals. *Faraday Discuss.* 2014, *167*, 389−403.

(21) Murray, B. J.; O'Sullivan, D.; Atkinson, J. D.; Webb, M. E. Ice nucleation by particles immersed in supercooled cloud droplets. *Chem. Soc. Rev.* 2012, *41*, 6519−6554.

(22) Pruppacher, H. R.; Klett, J. D.; Wang, P. K. Microphysics of Clouds and Precipitation. *Aerosol Sci. Technol.* 1998, *28*, 381−382.

(23) Sear, R. P. Nucleation: theory and applications to protein solutions and colloidal suspensions. *J. Phys.: Condens. Matter* 2007, *19*, 033101.

(24) Frenkel, D.; Smit, B. *Understanding Molecular Simulation: From Algorithms to Applications*; Elsevier (formerly published by Academic Press), 2002; Vol. *1*, pp 1−638.

(25) Abraham, F. *Homogeneous Nucleation: The Pretransition Theory of Vapor Condensation*; Academic Press: New York, 1974.

(26) Sholl, C.A; Fletcher, N. H. Decoration criteria for surface stepsCriteres de decoration pour les marches de surfaceDekoration- skriterien für oberflächenstufen. *Acta Metall.* 1970, *18*, 1083.

(27) Vali, G.; DeMott, P. J.; Möhler, O.; Whale, T. F. Technical note: A proposal for ice nucleation terminology. *Atmos. Chem. Phys.* 2015, *15*, 10263−10270.

(28) Chen, J.; Pei, X.; Wang, H.; Chen, J.; Zhu, Y.; Tang, M.; Wu, Z. Development, Characterization, and Validation of a Cold Stage-Based Ice Nucleation Array (PKU-INA). *Atmosphere* 2018, *9*, 357.

(29) Pruppacher, H. R.; Klett, J. D. *Microphysics of Clouds and Precipitation*, 2nd ed.; Kluwer Academic Publishers: New York, 1997.

(30) Alimi, O. S.; Farner Budarz, J.; Hernandez, L. M.; Tufenkji, N. Microplastics and Nanoplastics in Aquatic Environments: Aggrega- tion, Deposition, and Enhanced Contaminant Transport. *Environ. Sci. Technol.* 2018, *52*, 1704−1724.

(31) Herbort, A. F.; Schuhen, K. A concept for the removal of microplastics from the marine environment with innovative host-guest relationships. *Environ. Sci. Pollut. Res.* 2017, *24*, 11061−11065.

(32) Balakrishnan, G.; Deitel, M.; Nicolai, T.; Chassenieux, C.; Lagarde, F. Towards more realistic reference microplastics and nanoplastics: preparation of polyethylene micro/nanoparticles with a biosurfactant. *Environ. Sci.: Nano* 2019, *6*, 315−324.

(33) de Souza Machado, A. A. S.; Kloas, W.; Zarfl, C.; Hempel, S.; Rillig, M. C. Microplastics as an emerging threat to terrestrial ecosystems. *Glob Chang Biol.* 2018, *24*, 1405−1416.

(34) Oliveira, M.; Almeida, M.; Miguel, I. A micro(nano)plastic boomerang tale: A never ending story? *TrAC, Trends Anal. Chem.* 2019, *112*, 196−200.

(35) https://www.nationalgeographic.com/environment/2019/04/microplastics-pollution-falls-from-air-even-mountains/ (accessed April 15, 2019).

(36) Mattsson, K.; Hansson, L.-A.; Cedervall, T. *Nano-plastics in the aquatic environment* 2015, *17*, 1712−1721.

(37) https://waste4change.com/7-types-plastic-need-know/ (ac cessed August 4, 2019).

(38) Häusler, T.; Witek, L.; Felgitsch, L.; Hitzenberger, R.; Grothe, H. Freezing on a Chip − A New Approach to Determine Heterogeneous Ice Nucleation of Micrometer-Sized Water Droplets. *Atmosphere* 2018, *9*, 140.

(39) Lee, S.; Xu, H. Powder XRD and TEM study on crystal structure and interstratification of Zn-chlorite (baileychlore).

Powder Diffr. 2017, *32*, 118–123.

(40) Baruah, S.; Dutta, J. Hydrothermal Growth of ZnO Nanostructures. *Sci. Technol. Adv. Mater.* 2009, *10*, 013001.

(41) Helveg, S.; Lopez-Cartes, C.; Sehested, J.; Hansen, P. L.; Clausen, B. S.; Rostrup-Nielsen, J. R.; Abild-Pedersen, F.; Norskov, J. K. Atomic-Scale Imaging of Carbon Nanofibre Growth. *Nature* 2004, *427*, 426–429.

(42) Chong, E.; King, M.; Marak, K. E.; Freedman, M. A. The Effect of Crystallinity and Crystal Structure on the Immersion Freezing of Alumina. *J. Phys. Chem. A* 2019, *123*, 2447–2456.

(43) Wang, J.; Liu, X.; Milcovich, G.; Chen, T. – Y.; Durack, E.; Mallen, S.; Ruan, Y.; Weng, X.; Hudson, S. P. Co-reductive fabrication of carbon nanodots with high quantum yield for bioimaging of bacteria. *Beilstein J. Nanotechnol.* 2018, *9*, 137–145.

(44) Tobo, Y. An improved approach for measuring immersion freezing in large droplets over a wide temperature range. *Sci. Rep.* 2016, *6*, 32930.

(45) Kanji, Z. A.; Ladino, L. A.; Wex, H.; Boose, Y.; Burkert-Kohn, M.; Cziczo, D. J.; Kramer, M.; et al. Overview of. Ice Nucleating Particles. *Meteorol. Monogr.* 2017, *58*, 1.1–1.33.

(46) Hoose, C.; Moehler, O. Heterogeneous Ice Nucleation on Atmospheric Aerosols: a Review of Results from Laboratory Experiments. *Atmos. Chem. Phys.* 2012, *12*, 9817–9854.

(47) Chen, J.; Wu, Z.; Augustin-Bauditz, S.; Grawe, S.; Hartmann, M.; Pei, X.; Liu, Z.; Ji, D.; Wex, H. Ice nucleating particle concentrations unaffected by urban air pollution in Beijing, China. *Atmos. Chem. Phys.* 2018, *18*, 3523–3539.

(48) Oliani, W. L.; Parra, D. F.; Lima, L. F. C. P.; Lugao A. B. Effects of Thermal Ageing on HMS-PP Crystallinity. *2009 Interna- tional Nuclear Atlantic Conference*, INAC 27.09.2009-02.10.2009, Rio de Janeiro, Brazil, ISBN: 978-85-99141-03-8.

(49) Frei, E. R.; Ghazoul, J.; Pluess, A. R. Plastic responses to elevated temperature in low and high elevation populations of three grassland species. *PLoS One* 2014, *9*, No. e98677.

(50) https://www.lakeproductscompany.com/products/-artificial- seawater-astm-d- 1141- 98?gclid=EAIa IQobCh MIiMKs_ cDp4QIV1QOGCh2EQgCOEAAYAiAAEgL9XfD_BwE (accessed May 14, 2019).

(51) Junge, K.; Swanson, B. D. High-Resolution Ice Nucleation Spectra of Sea-Ice Bacteria: Implications for Cloud Formation and Life in Frozen Environments. *Biogeosciences* 2008, *5*, 865–873.

(52) Koop, T.; Zobrist, B. Parameterizations for Ice Nucleation in Biological and Atmospheric Systems. *Phys. Chem. Chem. Phys.* 2009, *11*, 10839–10850.

(53) Fitzner, M.; Sosso, G. C.; Cox, S. J.; Michaelides, A. The Many Faces of Heterogeneous Ice Nucleation: Interplay Between Surface Morphology and Hydrophobicity. *J. Am. Chem. Soc.* 2015, *137*, 13658–13669.

(54) Rios Mendoza, L. M.; Karapanagioti, H.; Alvarez, N. R. Micro (nanoplastics) in the marine environment: Current knowledge and gaps. *Environmental Science & Health* 2018, *1*, 47–51.

(55) Li, J. H.; Liu, X. R.; Zhang, Y.; Tian, F. F.; Zhao, G. Y.; Yu, Q. L. Y.; Jiang, F. L.; Liu, Y. Toxicity of nano zinc oxide to mitochondria. *Toxicol. Res.* 2012, *1*, 137–144.

(56) Shen, Y.; Chen, Z.; Hou, Z.; Li, T.; Lu, X. Ecotoxicological effect of zinc oxide nanoparticles on soil microorganisms. *Front. Environ. Sci. Eng.* 2015, *9*, 912–918.

(57) Liu, J.; Kang, Y.; Yin, S.; Song, B.; Wei, L.; Chen, L.; Shao, L. Zinc oxide nanoparticles induce toxic responses in human neuro- blastoma SHSY5Y cells in a size-dependent manner. *Int. J. Nanomed.* 2017, *12*, 8085–8099.

(58) Ganguly, M.; Dib, S.; Kurien, U.; Rangel-Alvarado, R. B.; Miyahara, Y.; Ariya, P. A. Influence of Environmentally Relevant Physicochemical Conditions on a Highly Efficient Inorganic Ice Nucleating Particle. *J. Phys. Chem. C* 2018, *122*, 18690–18704.

(59) Welti, A.; Kanji, Z. A.; Luönd, F.; Stetzer, O.; Lohmann, U. Exploring the Mechanisms of Ice Nucleation on Kaolinite: From Deposition Nucleation to Condensation Freezing. *J. Atmos. Sci.* 2014, *71*, 16–36.

(60) Wex, H.; DeMott, P. J.; Tobo, Y.; Hartmann, S.; Rosch, M.; Clauss, T.; Tomsche, L.; Niedermeier, D.; Stratmann, F. Kaolinite Particles as Ice Nuclei: Learning from the Use of Different Kaolinite Samples and Different Coatings. *Atmos. Chem. Phys.* 2014, *14*, 5529–5546.

(61) Ganguly, M.; Dib, S.; Ariya, P. A. Purely Inorganic Highly efficient Ice Nucleating Particles. *ACS Omega* 2018, *3*, 3384–3395.

(62) Sadeghi, A.; Imanpoor, M. R. Acute Toxicity of Mercuric Chloride (HgCl₂), Lead Chloride (PbCl₂) and Zinc Sulfate (ZnSO₄) on Silver Dollar Fish (Metynnis fasciatus). *Iranian Journal of Toxicology* 2015, *9*, 1301–1306.

(63) Ganguly, M.; Dib, S.; Ariya, P. A. Fast, Cost-effective and Energy Efficient Mercury Removal Recycling Technology. *Sci. Rep.* 2018, *8*, 16255.

(64) Eeshwarasinghe, D.; Loganathan, P.; Kalaruban, M.; Sounthararajah, D. P.; Kandasamy, J.; Vigneswaran, S. Removing polycyclic aromatic hydrocarbons from water using granular activated carbon: kinetic and equilibrium adsorption studies. *Environ. Sci. Pollut. Res.* 2018, *25*, 13511–13524.

(65) Yan, J.; Wang, L.; Fu, P. P.; Yu, H. Photo mutagenicity of 16 polycyclic aromatic hydrocarbons from the US EPA priority pollutant list. *Mutat. Res., Genet. Toxicol. Environ. Mutagen.* 2004, *557*, 99–108.

(66) Rangel-Alvarado, R. B.; Willis, C. E.; Kirk, J. L.; St Louis, V. L.; Amyot, M.; Belanger, D.; Ariya, P. A. Athabasca Oil Sands Region Snow Contains Efficient Micron and Nano-sized Ice Nucleating Particles. *Environ. Pollut.* 2019, *252*, 289–295.

(67) de Souza Machado, A. A.; Kloas, W.; Zarfl, C.; Hempel, S.; Rillig, M. C. Microplastics as an emerging threat to terrestrial ecosystems. *Global Change Biology* 2018, *24*, 1405–1416.

(68) Ariya, P. A.; Dastoor, A.; Nazarenko, Y.; Amyot, M. Do snow and ice alter urban air quality? *Atmos. Environ.* 2018, *186*, 266–268.

(69) Hasenkopf, C. A.; Veghte, D. A.; Schill, G. P.; Lodoysamba, S.; Freedman, M. A.; Tolbert, M. A. Ice nucleation, shape, and composition of aerosol particles in one of the most polluted cities in the world: Ulaanbaatar, Mongolia. *Atmos. Environ.* 2016, *139*, 222–229.

(70) Côté, V.; Kos, G.; Mortazavi, R.; Ariya, P. A. Microbiological transformation of dicarboxylic acids by airborne fungi. *Sci. Total Environ.* 2008, *390*, 530−537.

(71) https://www.telegraph.co.uk/news/2019/02/04/microplastics- glued-together-ocean-bacteria-making-big-enough/(accessed August 9, 2019).

(72) Voisin, D.; Jean-Luc Jaffrezo, J.−L.; Houdier, S.; Barret, M.; Cozic, J.; King, M. D.; France, J. L.; Reay, H. J.; Grannas, A.; Kos, G.; Ariya, P. A.; Beine, H. J.; Domine, F. Carbonaceous species and humic like substances (HULIS) in Arctic snowpack during OASIS field campaign in Barrow. *Journal of Geophysical Research: Atmospheres* 2012, *117*, DR00R19.